Assessing temporal variations of Ammonia Nitrogen concentrations and loads in the Huaihe River Basin in relation to policies on pollution source control

Xu, Jing, Jin, Guangqiu, Tang, Hongwu, Zhang, Pei, Wang, Shen, Wang, You-Gan and Li, Ling

Xu, J,., Jin, G., Tang, H., Zhang, P., Wang, S., Wang, Y.-G. and Li, L. (2018). Assessing temporal variations of Ammonia Nitrogen concentrations and loads in the Huaihe River Basin in relation to policies on pollution source control. *Science of the Total Environment, 642*, pp. 1386-1395. https://doi.org/10.1016/j.scitotenv.2018.05.395

Temporal patterns in concentration, loads and sources apportionment of Ammonia Nitrogen in the Middle Reaches of Huaihe River, from 1998 to 2013

Jing Xu [1,2], Guangqiu Jin[1,2]*, Hongwu Tang[1,2], Pei Zhang[1,2], Shen Wang, You-Gan Wang[4], Ling Li[1,3], D. A. Barry[5]

[1] State Key Laboratory of Hydrology-Water Resources and Hydraulic Engineering, Hohai University, Nanjing, China

Emails: xujinghhu@hhu.edu.cn, jingq@hhu.edu.cn, hwtang@hhu.edu.cn

[2] Centre for Eco-Environmental Modelling, College of Water Conservancy and Hydropower Engineering, Hohai University, Nanjing, China

[3] School of Civil Engineering, University of Queensland, Queensland, Australia

Email: l.li@uq.edu.au

[4] School of Mathematical Sciences, Queensland University of Technology, Queensland, Australia

Email: you-gan.wang@qut.edu.au

[5] Laboratoire de technologie écologique, Institut d'ingénierie de l'environnement, Faculté de l'environnement naturel, architectural et construit (ENAC), Ecole Polytechnique Fédérale de Lausanne (EPFL), Station 2, 1015 Lausanne, Switzerland

Email: andrew.barry@epfl.ch

Abstract

The Huaihe River Basin (HRB) is an important basin in eastern China which has been suffering from serious water pollution. In this paper, we analyzed the temporal patterns of ammonia nitrogen (AN) concentration, loads and sources apportionment in the middle reaches of Huaihe River (MRHR), including main stream of Huaihe River (MSHR) and two major tributaries, Shaying River (SR) and Guo River (GR), from 1998 to 2013. A modified log-linear model that takes the specific seasonal patterns of the MRHR into account has been developed. The modification is necessary to account for the decreasing ranges and amplitudes of the seasonal cycles over the years which are pretty important in the MRHR but were neglected in the former research. This model also plays an important role in obtaining regular daily AN concentration value from the irregular sampled concentration data for total loads estimation. The AN concentration showed a significant decrease while the annual decline rate ranged from 8.3% to 10.5% in the MSHR and more than 17% in the SR and GR. However, rebounds existed in AN flow-weighted concentration in the first year of all Five-Year Plans (measures for controlling water pollution). The AN loads showed a decreasing tendency but some rebounds occurred in the MSHR which mainly related to magnitude changes in annual flow. The AN loads from point sources had decreased from 50~81% to 3~13% in the MSHR and dropped from 74~93% to 3~28% in the SR and GR. Besides, extreme high AN concentration values (sudden water pollution accidents) usually occurred in wet seasons. So, in order to further decrease the AN concentration, governments could have more initiatives in making stricter upper limitation of contaminants loads during wet seasons, implementing measures for controlling water pollution continuously, reducing non-point sources pollution, carrying out scientific sluice regulation and joint pollution prevention programs in future measures for controlling water pollution.

Keywords: Middle Reaches of Huaihe River, Ammonia Nitrogen, modified log-linear model, temporal patterns, measures for controlling water pollution

1 Introduction

Degradation of water quality resulting from excessive contaminants loads which are far more than water environment capacity has become a global problem and causes serious consequences, like eutrophication, acidification and hypoxia [*Bocaniov and Scavia*, 2016; *Park et al.*, 2015; *Williams et al.*, 2015]. The Huaihe River Basin (HRB) which is an important basin in eastern China has been suffering from severe water pollution [*Wang et al.*, 2014] mainly due to seasonal water shortage and anthropogenic activities like rapid urbanization, intensive industrial and agricultural activities, and changes in land use/ land cover (LULC) [*He et al.*, 2015; *Water pollution prevention and control plan for the Huai River Basin (1997-2000)*, 1996]. Several large-scale water pollution accidents happened in the HRB and approximate 10 million residents were suffering from unsafe drinking water [*Jiang et al.*, 2011], especially from 1992 to 1995 [*Chu*, 1993; *Zhao*, 2015; *Zhu*, 1992]. Besides, the HRB is the place where has highest cancer incidence in China [*Tian et al.*, 2013; *Zhang et al.*, 2013]. All these posed obstacles in regionally social and economic development and drew governments' great concerns. Therefore, measures started to carry out to combat with water pollution in the HRB in 1997, called ninth (1997~2000), tenth (2001~2005), eleventh (2006~2010) and twelfth (2011~2015) Five-Year Plan (FYP) separately. During this period, several measures were applied to reduce point sources emission, such as close highly polluted factories, construct sewage treatment plants and set seasonally upper limitation of contaminants loads that are allowed to discharge into water body [*Water pollution prevention and control plan for the Huai River Basin (1997-2000)*, 1996; *Water* *pollution prevention and control plan for the Huai River Basin (2001-2005)*, 2000; *Water pollution prevention and control plan for the Huai River Basin (2006-2010),* 2006; *Water pollution prevention and control plan for the Huai River Basin (2011-2015),* 2010].

Previous research found that water quality has improved significantly in the HRB after 2000s due to implementation of measures for controlling water pollution [*Dou et al.*, 2016; *Tong et al.*, 2015]. Meanwhile, ammonia nitrogen (AN) has become the most severe pollution in the HRB, especially in two major tributaries, Shaying River (SR) and Guo River (GR) [*Dou et al.*, 2016; *Jiang et al.*, 2011; *Liu*, 2009; *Zhai et al.*, 2014]. Considering that many tributaries flow into the middle reaches of the Huaihe River (MRHR) and this area is intensively interrupted by anthropogenic activities [*Zhai et al.*, 2014], we focused on analyzing temporal patterns of AN in the MRHR in this paper, including the main stream of Huaihe River (MSHR) and two major tributaries, SR and GR. However, the previous research had a huge deficiency in that they analyzed the original water quality dataset directly and ignored biases that may cause because it is a common sense that samples tend to be collected more frequently during wet-seasons and sudden water pollution accidents [*Wang and Tian*, 2013; *Wang et al.*, 2011]. This means that we should find an appropriate model to regress irregular sampling data to obtain interpolated daily concentration data before analyzing. Model to describe the temporal patterns of water quality concentration considering long-term trend, seasonality of concentration data was firstly developed as a log-linear model based on the ‘rating curves’ [*Colby*, 1956; *Miller*, 1951; *Thompson*, 1987; *Young and Depinto*, 1988], then the seven-parameter model was proposed [*Cohn et al.*, 1992]. In order to consider the influence of historical flow, the conception of average discounted flow (ADF) was proposed [*Wang and Tian*, 2013; *Wang et al.*, 2011]. *Zhang and Ball* [2017] found that the effectiveness of ADF is superior that other terms considering the historical influence of flow in nutrients loads estimation. However, because of significant decrease of AN concentration and complex seasonal patterns due to intensive anthropogenic activities [*Dou et al.*, 2016; *Zhai et al.*, 2014], previous log-linear model may not be sufficient to describe temporal patterns of AN concentration in the HRB. In order to develop the modified model, the Seasonal Trend decomposition using Loess (STL) [*Cleveland et al.*, 1990] method will be used to extract seasonal component, which is used widely in analysis of nutrient concentration [*Qian et al.*, 2000; *Stow et al.*, 2015; *Stow et al.*, 2014; *Wan et al.*, 2017], suspended sediment concentration[*Lamon et al.*, 2004] and water level [*Sellinger et al.*, 2008; *Shamsudduha et al.*, 2009]. Then seasonal periods were extracted by the Fast Fourier Transform (FFT) [*Iwashita and Shimamura*, 2003], which is the computationally efficient means to calculate the Discrete Fourier Transform (DFT) [*Dilmaghani et al.*, 2007].

The objects of this paper are to (1) develop a modified log-linear model which incorporates varying seasonal patterns of AN concentration in the MRHR for the purpose of obtaining daily and regular concentration values from the AN concentration data sampled irregularly to obtain interpolated daily values; (2) analyze temporal patterns in AN concentration, loads and sources apportionment from 1998 to 2013 in the MRHR; (3) evaluate the effectiveness and weakness in measures for controlling AN pollution in the MRHR. Our research is expected to provide a scientific basis for implementation of measures for controlling water pollution in future and guarantee water security and sustainable development in the MRHR.

2 Materials and methods

2.1 Study area and sampling stations

Huaihe River is one of the most important rivers in eastern China, locating between latitudes 30°~36°N and longitudes 111°~121°E, with the basin area of 270,000 km^2. Huaihe River originates from the Tongbai Mountain in Henan Province, passing Henan, Anhui and Jiangsu Province from west to east before flowing into the Hongze Lake [*Zhai et al.*, 2014; *Zhang et al.*, 2013]. The research area in this paper is the middle reaches of Huaihe River (MRHR), including main stream of Huaihe River (MSHR) and two major tributaries, Shaying River (SR) and Guo River (GR) (Fig. 1).

There are ten monitoring stations in the MRHR which have weekly or monthly sampling AN concentration dataset and daily flow dataset. The time scale of AN concentration in S5, S8, S9 and S10 is from 2003 to 2013 which is from 1998 to 2013 in other stations (Table 1). As flow data series is long enough to match with the concentration data, research period in this paper is selected to be from 1998 (or 2003) to 2013. AN concentration dataset used in this paper was provided by monitoring center of Huai River Water Resources Protection Bureau and flow dataset was from hydrographic office of Huaihe River Basin Commission. The concentration of AN was tested by the national standard of water quality testing [*Water quality-Determination of ammonia nitrogen-Distillation-neutralization titration*, 2010]. Besides, mass of AN from sewage outfall was available during the period from 2000 to 2013, including industrial and urban domestic sewage discharge.

2.2 Methods

In order to describe the specific seasonality of AN concentration in the MRHR to develop the modified log-linear regression model, the seasonal component of AN concentration should be analyzed first. The Seasonal Trend decomposition using Loess (STL) [*Cleveland et al.*, 1990] method was used to extract long-term trend and seasonality of AN concentration. The STL method is an iterative nonparametric procedure based on a locally weighted regression (LOESS) [*Cleveland*, 1979; *Cleveland and Devlin*, 1988] to extract the low-frequency long-term tendency, high-frequency seasonality and residuals components from time series. It consists of inner loops and outer loops. The trend component is decomposed by a continuous loess line and seasonal component is decomposed by 12 month-specific loess line in inner loops. Robust estimates are used in outer loops to keep the long-term trend and seasonal components away from being distorted by outliers. The iterative fitting ends when all components are convergent. By using the STL model, observed concentration values can be decomposed as:

$$C = C_T + C_S + C_R \tag{1}$$

where C is value of monthly average of observed concentration (mg L^{-1}), C_T is trend component (mg L^{-1}), C_S is seasonal component (mg L^{-1}), C_R is residual which cannot be explained by long-term tendency and seasonality (mg L^{-1}). There are two smooth parameters that represent the window widths of trend and seasonal components. In this paper, seasonal window was chosen to be 21 and trend window to be 9 (time series from 2003 to 2013) or 11 (time series from 1998 to 2013) following the suggestions in *Cleveland et al.* [1990]. However, the STL fails to provide a useful way to test whether the increase or decrease tendency in the long-term trend component is significant, thus we will use the analysis of variance (ANOVA) and Student's t test to compensate.

The Fast Fourier Transform (FFT) [*Iwashita and Shimamura*, 2003] was used to obtain seasonal periods from seasonal component of AN concentration extracted from the STL. The FFT is the most efficient way to calculate the Discrete Fourier Transform (DFT) in computers, which can reveal periods (1/frequencies) and relative strengths (amplitudes) of corresponding periods. In spectrograms, seasonal periods can be determined by the frequencies corresponded to peak points. However, in order to reach a compromise between accuracy and complexity of the modified model, amplitudes of all peak points in each station was ordered and these frequencies whose amplitudes account for 80% of total amplitudes (Fig. 3) were chosen and included in the modified model.

Our modified log-linear model was based on the model from *Wang and Tian* [2013]:

$$\begin{aligned}\ln(\mathrm{C}) = \beta_0 + \beta_1 \ln(\mathrm{ADF}) + \beta_2 \ln(\mathrm{Q}) + \beta_3[\ln(\mathrm{Q})]^2 + \beta_4 \sin(2\pi \mathrm{T}) + \beta_5 \cos(2\pi \mathrm{T}) \\ + \beta_6 \sin(4\pi T) + \beta_7 \cos(4\pi \mathrm{T}) + \varepsilon\end{aligned} \quad (2)$$

where Q is the flow ($\mathrm{m}^3\ \mathrm{s}^{-1}$), T is time (year), β_i is fitting coefficient, and ε is the error which is independent and normally distributed with zero mean.

The ADF is defined as:

$$ADF(\mathrm{d}) = \frac{(\mathrm{Q}_j + \mathrm{d}\mathrm{Q}_{j-1} + \ldots + \mathrm{d}^{j-1}\mathrm{Q}_1)}{(1 + \mathrm{d} + \ldots + \mathrm{d}^{j-1})}, \quad (3)$$

where Q_1 to Q_j represents the flow (m^3 s^{-1}) in day 1 to day *j*, and *d* is the discount factor ranging from 0.1 to 1, large *d* values indicate long lagged effects from the history flow. *Wang and Tian* [2013] suggested that *d* set to be 0.97/day in their data analysis.

Our modified model includes decrease trend and complex periods in seasonal component of AN concentration:

$$\begin{aligned}\ln(\mathrm{C}) = \beta_0 + \beta_1 \ln(\mathrm{ADF}) + \beta_2 \ln(\mathrm{Q}) + \beta_3[\ln(\mathrm{Q})]^2 + \beta_4 T + \\ (\beta_5 T + \beta_6) \times \{\textstyle\sum_{i=1}^{k} [\beta_{5+2i} \sin(2\mathrm{i} \times \pi \mathrm{T}) + \beta_{6+2i} \cos(2\mathrm{i} \times \pi \mathrm{T})]\} + \varepsilon\end{aligned} \tag{4}$$

Here the index *i* taking values 1, 2 and 3 representing periods of 12, 6 and 4-month, respectively. In our analysis, *k* is determined by the observed seasonal trends and it varies from station to station.

In this paper, Pearson's correlation coefficient ρ, adjusted R^2 (taking account of the number of parameters in the model [*Wherry*, 1931]) are used to evaluate the goodness-of-fit of linear models. Non-linear models are evaluated by Nash-Sutcliffe efficiency coefficients (NSE) [*Nash and Sutcliffe*, 1970]. According to guidelines [*Moriasi et al.*, 2007], NSE>0.5 indicates that model is acceptable. Outliers in regression were tested by Cook's distance and DFFITS criterion. If Cook's distance or DFFITS criterion of day *i* is larger than $\frac{4}{n-k-1}$ or $\sqrt{\frac{2(k+1)}{n}}$, the concentration in day *i* is considered as an outlier. All analysis was performed in R.3.2.3, which is a well-known program in statistical analysis.

3 Results and discussion

3.1 Long-term tendency and seasonality of AN concentration

Trend, seasonal and residuals components were obtained from average monthly AN concentration decomposed by the STL method. In Figure 2, the four panels are average monthly AN concentration, trend, seasonality, and residuals from left to right respectively.

Trend components in all stations present a decrease tendency while obvious high concentration period happened in S1 in 1999, S3 in 2003 and S5 in 2007, which is similar to the results in *Dou et al.* [2016] that AN concentration had fluctuations in early years. The three high concentration could be caused by low flow [*Liu*, 2009; *Tong et al.*, 2015]. According to *Water Resources Bulletin in the Huaihe River Basin* [1999], rainfall in wet season in 1999 was less than that in normal years by 43%. Thus, without enough flow to dilute, extreme high concentration happened when wastewater containing high AN concentration discharged into the MRHR.

Seasonal components in all stations displayed complex periods while the most remarkable period is 12-month period. The FFT was used to extract periods in seasonality. According to spectrograms (Fig. 3), frequencies whose amplitudes account for 80% of total were chosen in each station and turned to periods (1/ frequency) (Table 2). The most remarkably 12-month period in all stations can be seen as fundamental, and different stations had different periods in harmonics. Two reasons can explain the complex seasonal periods in AN concentration. Firstly, measures for controlling water pollution focused on decline point sources emission like set seasonally upper limitation of contaminants loads that are allowed to discharge into water body [*Water pollution prevention and control plan for the Huai River Basin (1997-2000)*, 1996; *Water pollution prevention and control plan for the Huai River Basin (2001-2005)*, 2000;

Water pollution prevention and control plan for the Huai River Basin (2006-2010), 2006; *Water pollution prevention and control plan for the Huai River Basin (2011-2015)*, 2010], which caused anthropogenic seasonal periods in AN concentration. Second, fertilizing nitrogen is mostly applied in spring and autumn during when are growth seasons in the MRHR. Moreover, flow has seasonal distribution in the HRB which can dilute AN concentration in water body [*Dou et al.*, 2016] and can carry AN loads from non-point sources. In addition, nature log transform of seasonal amplitudes displayed monotonous decrease trend in all stations except S3, S5, and S9 (Fig. 4). Therefore, AN concentration dataset in these three stations will be separated into two part at 2006, 2008 and 2008 respectively in regression.

Residuals components centered at 0 except the conditions that extreme high concentration happened. These extreme values in concentration may be caused by sudden water pollution accidents, which happened randomly and cannot be explained by long-term trend and seasonality.

3.2 Regression Analysis

The modified log-linear model (Eq. 4) was used to regress and interpolate sampling data to get daily AN concentration. Since detection limit (DL) of AN concentration is 0.025 mg L^{-1} and there are three values below DL in S2, one value in S5, S6 and S7, these data were replaced by 0.0125 mg L^{-1} and 0.025 mg L^{-1} separately in regression. The interpolated daily concentration values are pretty close and Pearson's correlation coefficients ρ are all higher than 0.999. Thus, the concentration values below the DL were chosen to be replaced by 0.0125 mg L^{-1} in this paper.

Compared the goodness of fit of the previous model (Eq. 2) and modified model (Eq. 4), an increase was found in adjusted R^2 from 0.530±0.156 to 0.609±0.120 (Table 2). Pearson's correlation coefficients ρ between observed and predicted values are from 0.64 to 0.87. Therefore, modified log-linear model can be judged to be satisfied and predicted daily concentration value is reliable for following analysis.

According to Cook's distance and DFFITS criterion, several outliers in regressions were found (Table 3). These outliers have the same feature that all observed values were remarkably higher than predicted ones, so it indicates that the outliers were caused by sudden water pollution accidents. There are two outliers happening in March in S1, S9 and one outlier in November in S8, during when are dry seasons in the HRB, while the others outliers all happened in wet seasons (May to September) in the HRB. According to the daily flow corresponding to the three outliers, it is reasonable to judge that these three extremely high values were the results of low flow, and a similar conclusion was found in *Liu* [2009] and *Tong et al.* [2015]. *Hagemann and Park* [2017] found that semi-parametric regression models fail to recognize the great effects of diluting contaminants under extremely high flow and tend to overpredict concentrations. This means that these outliers could be even more abnormal in wet seasons. Two reasons were responsible for sudden water accidents usually happened in wet seasons. Firstly, excess AN was discharged into water body during wet seasons. Strict seasonally upper limitation of AN loads from point sources were carried out in dry seasons. As high discharge can dilute AN concentration, limitation controls tend to relax a little in wet seasons. Also, some factories inclined to discharge wastewater without permission or beyond limitation during wet seasons because they thought magnitude of flow in this season is large enough to dilute highly polluted wastewater without causing water pollution accidents [*Sun and Yang*, 2013]. For example, according to *Water Resources Bulletin in the Huaihe River Basin* [1998], the outliers happening in S2, S3 and S4 in May 25, 1998 was caused by some factories in tributaries failed to meet the upper limitation of contaminants loads that allowed to discharge into waterbody. Then high polluted water flow into the MSHR caused sudden water pollution accident in S2, S3, S4 (fig. 6(a)). Second reason is that there are many sluices existing in the HRB to combat with water shortage condition in this area. Sluices were usually closed to guarantee water supply in dry seasons. Thus, highly polluted water was more likely to accumulate before these closed sluices. When wet seasons come and sluices open to discharge flood, highly polluted water was instantaneously discharged and caused sudden pollution accidents [*Jiang et al.*, 2011; *Zhai et al.*, 2014]. It also can be proved by daily flow values in the time when outliers happened. For example, in S5, the flow value in 2007/7/16 was 1230 m^3 s^{-1} and it was the first flood at that year, while the previous five-day-average flow was 336 m^3 s^{-1} (fig. 6(b)). In S6, the flow value in 2010/9/9 was 2740 m^3 s^{-1} and it was a flood peak, while the previous five-day-average flow was 866 m^3 s^{-1} (fig. 6(c)). This indicates that the outliers that happened in S5 and S6 were caused by discharging of large amount of flow containing high polluted contaminants. Therefore, in order to prevent happening of sudden water pollution accidents, stricter limitation of AN loads from sewage outfall and more rigorous monitoring of wastewater discharging from factories should be carried out by officials during wet seasons. Scientific sluice regulation and joint pollution prevention programs that consider both water quantity and quality [*Zhai et al.*, 2014] are also important in preventing sudden water accidents.

3.3 Temporal patterns of AN concentration

In order to test whether significant decrease of AN concentration had happened between each FYP, interpolated daily AN concentration dataset was separated into four parts according to time scale of each FYP. Variance of AN concentration in four parts was calculated and average AN concentration during each FYP was significantly unequal ($p<2\times10^{-16}$). Therefore, Student's t test was conducted for three times during four FYPs in each station to detect whether decrease in AN concentration is significant between each two FYPs. In order to reduce the probability of making a type I error, the Bonferroni method [*Qian*, 2010] was used to modify the α level:

$$\alpha_t = \frac{\alpha}{M} \quad , \qquad (5)$$

where α is origin level, *M* is the times conducting the Student's t test. In this case, because Student's t test was conducted for three times, α was set to be 0.05, so α_t was chosen to be 0.017.

In Table 4, the AN concentration in the SR and GR was largely higher than the MSHR during the ninth and tenth FYPs. With applying of measures for controlling water pollution, AN concentration had decreased remarkably in the MRHR. Gaps between MSHR and two major tributaries were narrowed. By the twelfth FYP, the largest gap was only 2mg/L because of huge decrease in AN concentration happening in the SR and GR. Decrease in AN concentration was significant ($p<0.017$) only between tenth and eleventh FYP in the MSHR and was significant ($p<0.017$) between all FYPs in two major tributaries, which is corresponding to the results in *Zhai et al.* [2014] that AN concentration decrease significantly in SR, GR. This implies that measures for controlling AN had more effects in two major tributaries than in the MSHR.

According to the climatic features in the HRB, we set March to May to be spring, June to August to be summer, September to November to be autumn and December to February to be winter. Then, decline rate of average annual and seasonal AN concentration was calculated (Table 5). Annual decline rates ranged from 8.3% to 10.5% in the MSHR and more than 17% in the SR and GR. AN concentration in winter displayed the highest decline rate than other seasons and concentration in summer displayed the lowest decline rate in the MSHR. While in the SR and GR, decline rate in four seasons was almost equal.

Average annual flow-weighted AN concentration is calculated by annual total AN loads divided by annual total flow (Eq. 6):

$$C_{FW} = \frac{\sum_{i=1}^{365} Q_i \times C_i}{\sum_{i=1}^{365} Q_i} \tag{6}$$

Flow-weighted AN concentration displayed a decrease tendency in general but rebounds always happened in the first year of FYPs (Fig. 7) expect S6 to S10 in twelfth FYP. These rebound rates present in Table 6, which are the largest in tenth FYP and all more than 100% in the MSHR. This rate declined a lot in the eleventh FYP and had a further decline in the twelfth FYP while AN flow-weighted concentration displayed no rebounds in S6 to S10 in the SR and GR. This rebound phenomenon may be caused by the discontinuity of measures' implementation in the process of each FYP.

3.4 Temporal patterns of AN loads and sources apportionment

Average annual AN loads were calculated by:

$$Load = \frac{1}{365}\sum_{i=1}^{365} Q_i \times C_i \tag{7}$$

AN loads showed a decrease tendency but some rebounds happened which were more often in the MSHR (Fig. 8). From the previous analysis, average annual AN concentration decreased significantly, so rebounds of loads related to the magnitude changes in annual flow, as high flow from surface can carry more fertilizing nitrogen.

The point sources of AN loads are mainly from sewage outfalls, including industrial and domestic wastewater. Because of data limitation, non-point sources of AN loads are considered to be fertilizing nitrogen carried by surface runoff. AN mass from sewage outfall has a decrease and amount of fertilizing nitrogen almost has no change from 2000 to 2013 (Fig. 9). Using an exponential model and a linear model to stimulate amount of AN mass of sewage outfalls and fertilizing nitrogen separately, the coefficient of exponential model is 0.10 and slope of linear model is 1.01, which indicates amount of fertilizing nitrogen usage can be considered as stable. Therefore, AN loads from non-point sources are only controlled by magnitude of flow. As AN loads from point sources were exponential decrease, Eq.8 can be used to describe the features of point and non-point sources of AN loads, which is a model used to describe two sources, one is changing with time and another stay stable[*Stow et al.*, 2004].

$$Load_i = \beta_1 \times e^{-k \times T} + \beta_2 \times \overline{Q_i} + \varepsilon \quad (8)$$

Where T is time, $\overline{Q_i}$ is average annual flow in i year, and $Load_i$ is average annual loads in year i. As Eq.8 is a non-linear model, Nash-Sutcliffe efficiency coefficient (NSE) is used to evaluate goodness-of fit of model. The fitting formla and NSE in each station present in table 7. All NSEs are higher than 0.76, which means Eq.8 to be satisfied. From this model, contribution of point and non-point sources can be calculated. The contributation of point sources has dropped from 50~81% to 3~13% in the MSHR and dropped from 74~93% to 3~28% in the SR and GR (Fig. 10), while *Zhai et al.* [2014] also pointed that non-point sources pollution were gradually becoming a prominent threat. It is corresponded to the measures for controlling water pollution which focus on cutting down the amount of AN from point sources emission. Meanwhile, decrease in contribution of point sources caused increase in contribution of non-point sources necessarily. Contribution of non-point sources was more than 50% after 2005 in the MSHR, especially, more than 90% in S3 and S4. Continuing to focus on controlling point sources will not be enough to make a further decrease in AN concentration. This is why decrease trend was no longer significant after the evelenth FYP in the MSHR. Contrubition of non-point sources in the SR and GR was less than the MSHR, thus, controlling point sources was still useful in SR and GR in decreasing AN concentration. However, contrubition of non-point sources was larger than 90% in S7 and S9, which seems to be a contracdiction. This is because there is a limitation existing in Eq. 8. While quantifying loads of non-point sources by flow, some loads from sewage outfalls had been included by mistake. Some factories alongside the SR and GR dischraged wastewater without permission or more than limitation during wet seasons to maximize their profits [*Sun and Yang*, 2013]. In this case, factories discharged more AN loads by sewage outfalls as flow increased, which has the same feasure as AN loads from non-point sources. Thus, monitoring factories near S7 and S9 shoule be paid more attention to, espically in wet seasons.

4 Conclusions

In order to provide scientific suggestions for implementation of measures for controlling water pollution in future and guarantee water security and sustainable development in the MRHR, we analyzed temporal patterns in AN concentration, loads and sources apportionment in the MRHR from 1998 to 2013. By results from the STL method and the FFT, a modified log-linear model was developed based on the previous loads estimation log-linear model to interpolate daily AN concentration values. Analyzing these daily AN concentration values, results obtained are summarized as following:

(1) Significant decrease in AN concentration happened between tenth to eleventh FYP in the MSHR and between all FYPs in the SR and GR. Annual decline rate of AN concentration ranged from 8.3% to 10.5% in the MRHR and more than 17% in the SR and GR.

(2) AN loads showed a decrease tendency but some rebounds happened in the

MSHR which related to magnitude changes in annual flow. As measures for controlling water pollution focused on cutting down AN from point sources, the contribution of point sources had decreased from 50~81% to 3~13% in the MSHR and dropped from 74~93% to 3~28% in the SR and GR. This implies that non-point sources are gradually becoming main sources of AN loads in the MRHR.

(3) Extreme high AN concentration values (sudden water pollution accidents) usually happened in wet seasons which were caused by two reasons. First, factories were tended to discharge polluted wastewater without permission or beyond limitation during wet seasons in the MRHR. Second, highly polluted water that accumulated before closed sluices in dry seasons was instantaneously discharged with the first flood during wet seasons.

(4) Rebounds in AN Flow-weighted concentration happened in the first year of each FYP except twelfth FYP in S6 to S10, which indicates that problems exist in the continuity in implementation of measures for controlling water pollution.

In order to obtain a further improvement in water quality in the HRB, governments should have more initiatives in making stricter upper limitation of contaminants loads during wet seasons, implementing measures for controlling water pollution continuously, reducing non-point sources pollution, carrying out scientific sluice regulation and joint pollution prevention programs in future measures for controlling water pollution.

Acknowledgments

This research was supported by the Natural Science Foundation of China (51239003, 51679065, 51421006). Data used in the analysis presented in the paper can be obtained by sending a request to the corresponding author (jingq@hhu.edu.cn).

References

Bocaniov, S. A., and D. Scavia (2016), Temporal and spatial dynamics of large lake hypoxia: Integrating statistical and three-dimensional dynamic models to enhance lake management criteria, *Water Resources Research*, *52*(6), 4247-4263.

Chu, J. T. (1993), Large scale water pollution happened again in main stream of Huiahe River, *Zhi Huai*, 3-5.

Cleveland (1979), Robust Locally Weighted Regression and Smoothing Scatterplots, *Journal of the American Statistical Association*, *74*(368), 829-836.

Cleveland, and S. J. Devlin (1988), Locally weighted regression: an approach to regression analysis by local fitting, *Journal of American Statostical Associatiom*, *83*(403), 596-610.

Cleveland, W. S. Cleveland, J. E. Mcrae, and I. Terpenning (1990), STL: a seasonal-trend decomposition procedure based on loess, *Journal of Official Statistics*, *6*(1), 3-73.

Cohn, T. A., D. L. Caulder, E. J. Gilroy, L. D. Zynjuk, and R. M. Summers (1992), The validity of a sample statistical model for estimating fluvial constituent loads: an empirical study involving nutrient loads entering Chesapeake Bay, *Water Resources Research*, *28*(9), 2353-2363.

Colby, B. R. (1956), Relationship of sediment discharge to streamflow, *Open-File Report*.

Dilmaghani, S., I. C. Henry, P. Soonthornnonda, E. R. Christensen, and R. C. Henry (2007), Harmonic analysis of environmental time series with missing data or irregular sample spacing, *Environ Sci Technol*, *41*(20), 7030-7038.

Dou, M., Y. Zhang, and G. Li (2016), Temporal and spatial characteristics of the water pollutant concentration in Huaihe River Basin from 2003 to 2012, China, *Environmental monitoring and assessment*, *188*(9), 522.

Hagemann, M., and M.-H. Park (2017), Capacity of semi-parametric regression models to predict extreme-event water quality in the Northeastern US, *Journal of Hydrology*, *547*, 575-584.

He, T., Y. Lu, Y. Cui, Y. Luo, M. Wang, W. Meng, K. Zhang, and F. Zhao (2015), Detecting gradual and abrupt changes in water quality time series in response to regional payment programs for watershed services in an agricultural area, *Journal of Hydrology*, *525*, 457-471.

Iwashita, M., and T. Shimamura (2003), Long-term variations in dissolved trace elements in the Sagami River and its tributaries (upstream area), Japan, *Science of The Total Environment*, *312*(1-3), 167-179.

Jiang, Y., Q.-d. Peng, H.-h. Luo, and M. Ma (2011), Analysis of spatial and temporal variation of water quality in Huiahe River Basin (in Chinese), *Journal of Hydraulic Engineering*, *42*(11), 1283-1288.

Lamon, E. C., S. S. Qian, and D. D. Richter (2004), Temporal changes in the Yadkin River flow versus suspended sediment concentration relationship, *Journal of the American Water Resources Association*, *40*(5), 1219-1229.

Liu, Y.-n. (2009), Study on spatial and temporal variation of water quality in middle reaches of Huaihe River, *Water Resources Protection*, *25*(4), 1-4.

Miller, C. R. (1951), Analysis of flow-duration, sediment-rating curve method of computing sediment yield, *U.s.bureau of Reclamation*.

Moriasi, D. N., J. G. Arnold, M. W. Van Liew, R. L. Bingner, R. D. Harmel, and T. L. Veith (2007), Model evaluation guidelines for systematic quantification of accuracy in watershed simulations, *Transactions Of the Asabe*, *50*(3), 885-900.

Nash, J. E., and J. V. Sutcliffe (1970), River flow forecasting through conceptual models part I — A discussion of principles, *Journal of Hydrology*, *10*(3), 282-290.

Park, Y., Y. A. Pachepsky, K. H. Cho, D. J. Jeon, and J. H. Kim (2015), Stressor–response modeling using the 2D water quality model and regression trees to predict chlorophyll-a in a reservoir system, *Journal of Hydrology*, *529*, 805-815.

Qian (2010), *Environmental and Ecological Statistics with R*, 117-154 pp., Chapman & Hall/CRC.

Qian, M. E. Borsuk, and C. A. Stow (2000), Seasonal and long-term nutrient trend decomposition along a spatial gradient in the Neuse River Watershed, *Environmental Science and Technology*, *34*(21), 4474-4482.

Sellinger, C. E., C. A. Stow, E. C. Lamon, and S. S. Qian (2008), Recent water level declines in the Lake Michigan-Huron syetem, *Environmental Science and Technology*, *42*, 367-373.

Shamsudduha, M., R. E. Chandler, R. G. Taylor, and K. M. Ahmed (2009), Recent trends in groundwater levels in a highly seasonal hydrological system: the Ganges-Brahmaputra-Meghna Delta, *Hydrology And Earth System Sciences*, *13*(12), 2373-2385.

Stow, E. C. Lamon, S. S. Qian, and C. S. Schrank (2004), Will Lake Michigan Lake trout meet the Great Lakes strategy 2002 PCB reduction goal?, *Environmental Science & Technology*, *38*, 359-363.

Stow, Y. Cha, L. T. Johnson, R. Confesor, and R. P. Richards (2015), Long-term and seasonal trend decomposition of Maumee River nutrient inputs to western Lake Erie, *Environmental Science and Technology*, *49*(6), 3392-3400.

Stow, et al. (2014), Phosphorus targets and eutrophication objectives in Saginaw Bay: A 35 year assessment, *Journal of Great Lakes Research*, *40, Supplement 1*, 4-10.

Sun, M.-q., and Z.-z. Yang (2013), The game analysis of environmental pollution treatment, *Green Economy*, 108-110.

Thompson, M. P. (1987), *Statistical Modelling of Sediment Concentration* The university of British Columbia.

Tian, D., et al. (2013), Dissolved microcystins in surface and ground waters in regions with high cancer incidence in the Huai River Basin of China, *Chemosphere*, *91*(7), 1064-1071.

Tong, Y., Y. Zhao, G. Zhen, J. Chi, X. Liu, Y. Lu, X. Wang, R. Yao, J. Chen, and W. Zhang (2015), Nutrient Loads Flowing into Coastal Waters from the Main Rivers of China (2006-2012), *Scientific reports*, *5*, 16678.

Wan, Y., L. Wan, Y. Li, and P. Doering (2017), Decadal and seasonal trends of nutrient concentration and export from highly managed coastal catchments, *Water research*, *115*, 180-194.

Wang, and T. Tian (2013), Sediment concentration prediction and statistical evaluation for annual load estimation, *Journal of Hydrology*, *482*, 69-78.

Wang, P. Kuhnert, and B. Henderson (2011), Load estimation with uncertainties from opportunistic sampling data – A semiparametric approach, *Journal of Hydrology*, *396*(1-2), 148-157.

Wang, T.-H. Chen, C.-Z. Zhu, and S.-C. Peng (2014), Trace organic pollutants in sediments from Huaihe River, China: Evaluation of sources and ecological risk, *Journal of Hydrology*, *512*, 463-469.

Water pollution prevention and control plan for the Huai River Basin (1997-2000) (1996), Ministry of Environmental Protection of the People Republic of China,, edited.

Water pollution prevention and control plan for the Huai River Basin (2001-2005) (2000), Ministry of Environmental Protection of the People Republic of China,, edited.

Water pollution prevention and control plan for the Huai River Basin (2006-2010) (2006), Ministry of Environmental Protection of the People Republic of China,, edited.

Water pollution prevention and control plan for the Huai River Basin (2011-2015) (2010), Ministry of Environmental Protection of the People Republic of China,, edited.

Water quality-Determination of ammonia nitrogen-Distillation-neutralization titration (2010), Ministry of Environmental Protection of the People's Republic of China,, edited.

Water Resources Bulletin in the Huaihe River Basin (1998), Ministry of Environmental Protection of the People Republic of China,, edited.

Water Resources Bulletin in the Huaihe River Basin (1999), Ministry of Environmental Protection of the People Republic of China,, edited.

Wherry, R. J. (1931), A New Formula for Predicting the Shrinkage of the Coefficient of Multiple Correlation, *Annals of Mathematical Statistics*, *2*(4), 440-457.

Williams, M. R., K. W. King, M. L. Macrae, W. Ford, C. Van Esbroeck, R. I. Brunke, M. C. English, and S. L. Schiff (2015), Uncertainty in nutrient loads from tile-drained landscapes: Effect of sampling frequency, calculation algorithm, and compositing strategy, *Journal of Hydrology*, *530*, 306-316.

Young, T. C., and J. V. Depinto (1988), Factors affecting the efficiency of some estiamtors of fluvial total phosphorous load, *Water Resources Research*, *24*(9), 1535-1540.

Zhai, X., J. Xia, and Y. Zhang (2014), Water quality variation in the highly disturbed Huai River Basin, China from 1994 to 2005 by multi-statistical analyses, *Science of The Total Environment*, *496*, 594-606.

Zhang, and W. P. Ball (2017), Improving riverine constituent concentration and flux estimation by accounting for antecedent discharge conditions, *Journal of Hydrology*, *547*, 387-402.

Zhang, G. Q. Wang, T. C. Pagano, J. L. Jin, C. S. Liu, R. M. He, and Y. L. Liu (2013), Using hydrologic simulation to explore the impacts of climate change on runoff in the Huaihe River Basin of China, *Journal of Hydrologic Engineering*, *18*(11), 1393-1399.

Zhao, C. Y. (2015), Huaihe River or bad river?, edited.

Zhu, H. K. (1992), Water pollution accident and treantment in main stream in Huaihe River in 1992, *Zhi Huai*, 25-27.

Table 1. Details of ten monitor stations in the MRHR, SR and GR.

Station Code	Station Name	Location	Time Scale	Concentration (mg L^{-1}) Mean	Concentration (mg L^{-1}) Standard Deviation	Number of Observations
S1	Wang Jiaba	MSHR	1998.1-2013.12	0.69	1.13	812
S2	Lu Taizi	MSHR	1998.1-2013.12	0.65	1.15	743
S3	Wu Jiadu	MSHR	1998.1-2013.12	1.22	1.53	211
S4	Xiao Liuxiang	MSHR	1998.1-2013.12	0.71	1.10	773
S5	Zhou Kou	SR	2003.1-2013.12	6.38	7.72	405
S6	Jie Shou	SR	1998.1-2013.12	3.54	6.27	876
S7	Fu Yang	SR	1998.1-2013.12	2.54	3.95	727
S8	Ying Shang	SR	2003.1-2013.12	1.88	2.44	701
S9	Guo Yang	GR	2003.1-2013.12	2.37	3.82	346
S10	Meng Cheng	GR	2003.1-2013.12	2.35	2.75	696

Table 2. Seasonal periods of AN concentration, adjusted-R^2 of former (R_1^2), modified log-linear model (R_2^2) and correlation coefficients (ρ) between observed and predicted value of modified log-linear model.

Station	Periods (month)	R_1^2	R_2^2	ρ
S1	12/6/2	0.504	0.552	0.74
S2	12/6/4/3	0.561	0.617	0.77
S3	12/6/3	0.390(1998-2006) 0.672(2007-2013)	0.472(1998-2006) 0.722(2007-2013)	0.64
S4	12/6/2	0.629	0.673	0.81
S5	12/6/4/3	0.226(2003-2008) 0.367(2009-2013)	0.404(2003-2008) 0.471(2009-2013)	0.61
S6	12/6/4/2	0.735	0.776	0.87
S7	12/6/2	0.728	0.757	0.87
S8	12/4/2	0.601	0.655	0.81
S9	12/6/4	0.407(2003-2008) 0.633(2009-2013)	0.611(2003-2008) 0.707(2009-2013)	0.77
S10	12/6/3/2	0.439	0.504	0.69

Table 3. Outliers of AN concentration from modified model. C_1 and C_2 represent observed and predicted value of AN concentration, respectively.

Station	Time	C_1 (mg L^{-1})	C_2 (mg L^{-1})
S1	2000/6/10	14.20	0.38
	2004/3/20	21.40	1.33
S2	1998/5/25	21.21	0.34
	1999/5/12	11.00	0.74
S3	1998/5/25	10.43	1.90
	2000/5/18	8.25	1.04
	2001/7/20	11.10	0.40
S4	1998/5/25	18.72	0.60
S5	2007/7/16	24.00	2.05
	2011/8/1	4.00	0.72
S6	2010/9/9	7.00	0.42
	2011/7/26	56.54	0.57
S7	2012/9/10	1.34	0.18
S8	2007/11/12	3.28	0.55
S9	2010/3/10	10.03	2.21

Table 4. Student's t test on AN concentration between two adjacent Five-Year Plans (FYPs) in ten monitor stations.

Station	M_1 (mg L^{-1})	M_2 (mg L^{-1})	M_3 (mg L^{-1})	M_4 (mg L^{-1})	P_{1-2}	P_{2-3}	P_{3-4}
S1	1.56±1.62	1.03±0.91	0.67±0.49	0.51±0.32	0.083	0.007***	0.067
S2	1.54±1.68	0.96±0.91	0.57±0.44	0.40±0.24	0.061	0.003***	0.018
S3	1.92±1.84	1.84±1.29	0.95±0.84	0.64±0.38	0.076	2×10^{-5}***	0.016
S4	1.84±2.04	1.19±1.26	0.69±0.67	0.47±0.41	0.090	0.008***	0.052
S5		9.94±5.13	5.66±3.85	2.45±1.59		6×10^{-5}***	2×10^{-7}***
S6	21.26±16.38	8.36±6.57	3.00±2.21	1.45±1.07	5×10^{-5}***	7×10^{-8}***	1×10^{-5}***
S7	14.02±11.92	6.14±5.26	2.20±1.99	1.02±0.96	5×10^{-4}***	7×10^{-7}***	2×10^{-4}***
S8		5.42±5.93	1.97±1.82	0.76±0.47		0.002***	6×10^{-6}***
S9		8.60±5.58	3.24±2.92	0.89±0.90		3×10^{-6}***	2×10^{-7}***
S10		6.20±4.34	2.59±1.60	1.05±0.34		2×10^{-5}***	6×10^{-10}***

M_1, M_2, M_3 and M_4 are average AN concentration in the period of the ninth, tenth, eleventh and twelfth FYP. P_{1-2}, P_{2-3} and P_{3-4} are the *p*-values of Student's t test of ninth to tenth FYP, tenth to eleventh FYP and eleventh to twelfth FYP, respectively. Asterisks mean that a significant (<0.017) decrease happened during these two FYPs.

Table 5. Annual decline rate of AN concentration in whole year and each season in ten monitor stations.

Station	D_{whole} (%)	D_{Spring} (%)	D_{Summer} (%)	D_{Autumn} (%)	D_{Winter} (%)
S1	8.3	3.6	3.9	9.7	10.8
S2	9.8	7.3	3.0	5.3	13.9
S3	9.2	9.3	6.1	10.4	9.8
S4	10.5	10.0	2.0	6.7	12.8
S5	17.1	17.9	26.2	16.9	12.2
S6	18.4	16.9	15.8	18.0	19.9
S7	18.5	19.8	17.4	15.9	17.5
S8	21.6	23.7	12.9	10.4	23.7
S9	24.9	25.9	29.2	28.0	22.4
S10	19.9	23.3	15.4	13.2	20.9

D_{whole}, D_{Spring}, D_{Summer}, D_{Autumn} and D_{Winter} represent annual decline rate of NN concentration in whole year and each season, respectively.

Table 6. Rebound rate in first year of tenth (2001), eleventh (2006) and twelfth (2011) FYP.

Station	2000~2001	2005~2006	2010~2011
S1	161.1%	56.5%	31.5%
S2	319.2%	65.8%	13.2%
S3	205.6%	40.2%	39.1%
S4	441.2%	93.4%	23.8%
S5		22.9%	2.0%
S6	62.7%	28.0%	-2.7%
S7	174.5%	47.9%	-0.3%
S8		39.8%	-21.2%
S9		14.6%	-29.5%
S10		8.9%	-18.3%

Table 7. Fitting formulas and Nash-Sutcliffe efficiency coefficient (*NSE*) of AN loads from point and non-point sources in ten monitor stations.

Station	Fitting formula	*NSE*
S1	$\mathrm{L} = 162e^{-0.186\times(t-1997)} + 0.405Q$	0.87
S2	$\mathrm{L} = 436e^{-0.214\times(t-1997)} + 0.341Q$	0.82
S3	$\mathrm{L} = 634e^{-0.232\times(t-1997)} + 0.782Q$	0.79
S4	$\mathrm{L} = 976e^{-0.566\times(t-1997)} + 0.415Q$	0.89
S5	$\mathrm{L} = 622e^{-0.184\times(t-2002)} + 1.727Q$	0.76
S6	$\mathrm{L} = 1504e^{-0.356\times(t-1997)} + 1.901Q$	0.91
S7	$\mathrm{L} = 3517e^{-0.617\times(t-1997)} + 1.724Q$	0.94
S8	$\mathrm{L} = 775e^{-0.293\times(t-2002)} + 0.520Q$	0.98
S9	$\mathrm{L} = 917e^{-0.766\times(t-2002)} + 2.372Q$	0.96
S10	$\mathrm{L} = 531e^{-0.564\times(t-2002)} + 1.696Q$	0.99

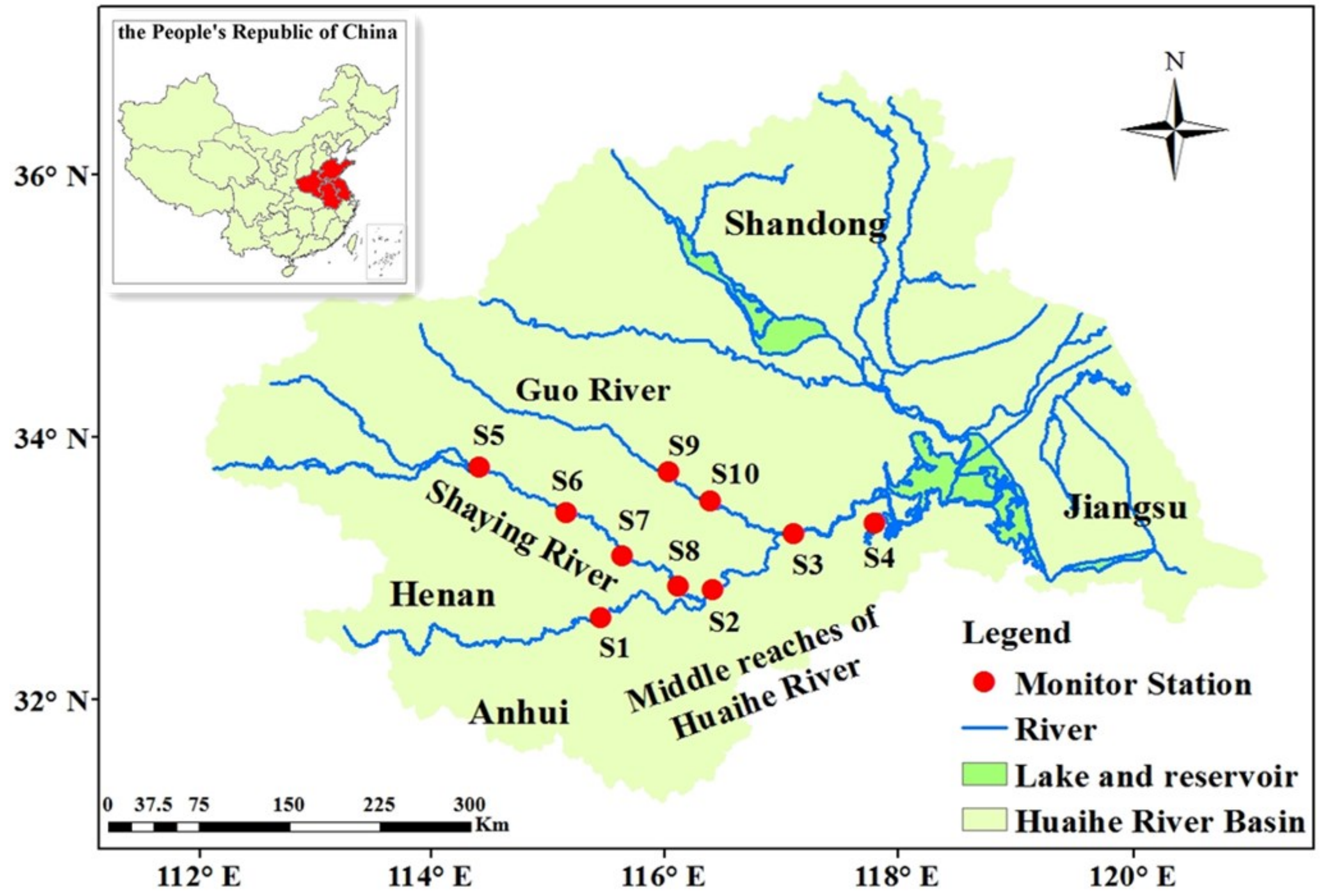

Figure 1. The Huaihe River Basin (HRB) locates in the east of the PRC, covering four provinces. Study area in this paper is the middle reaches of Huaihe River (MRHR), including two major tributaries, Shaying River (SR) and Guo River (GR). The ten monitor stations are shown by red points. Among them, S1 to S4 lie in the MRHR, S5 to S8 lie in the SR and S9 to S10 lie in the GR.

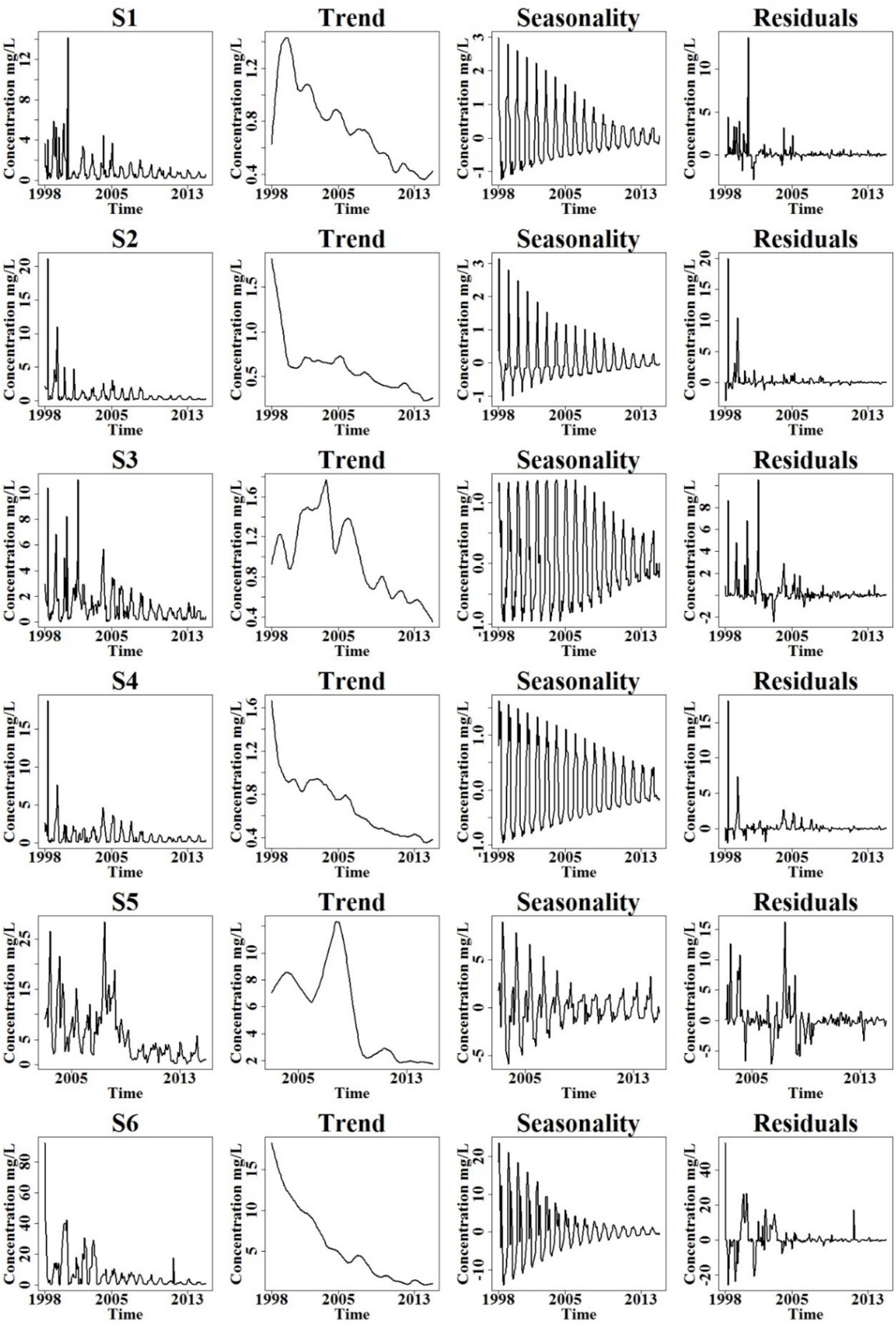
S1
Trend
Seasonality
Residuals
S2
Trend
Seasonality
Residuals
S3
Trend
Seasonality
Residuals
S4
Trend
Seasonality
Residuals
S5
Trend
Seasonality
Residuals
S6
Trend
Seasonality
Residuals
Concentration mg/L
Time

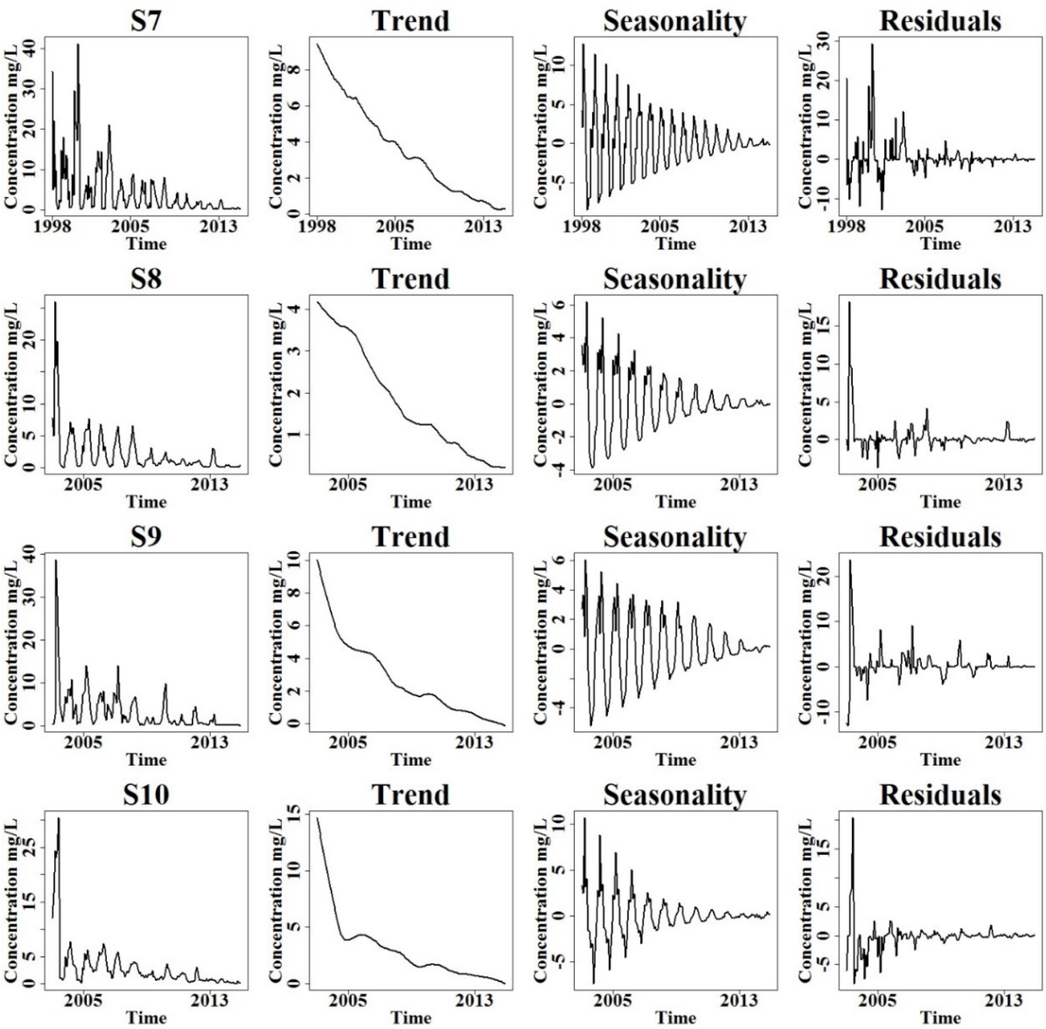

Figure 2. Average monthly AN concentration and three components decomposed by Seasonal trend decomposition using loess (STL) in ten monitor stations. From left to right, the four panels show average monthly AN concentration, long-term trend, seasonality, and residuals, respectively.

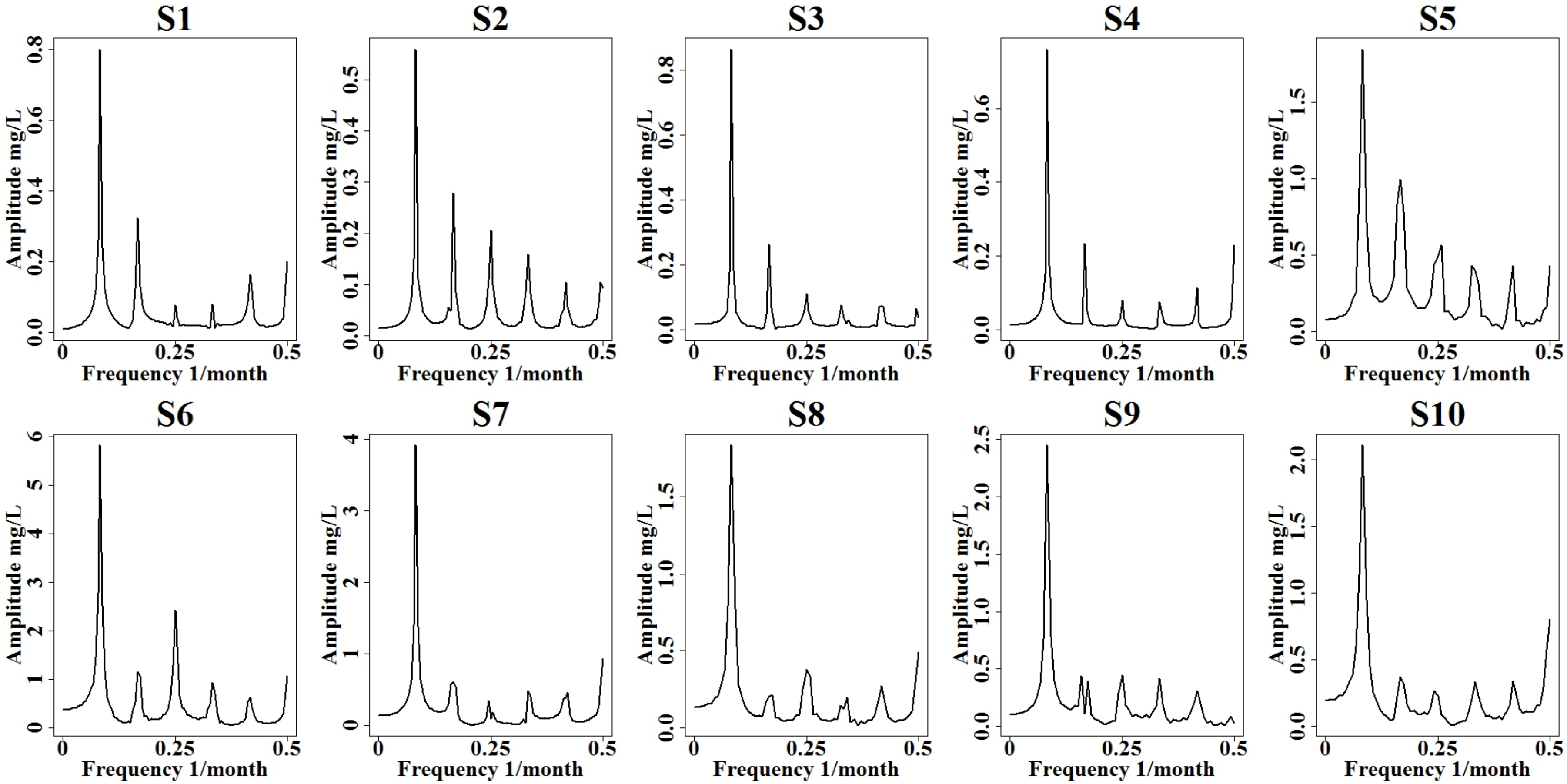

Figure 3. Spectrum analysis of seasonal components of AN concentration in ten monitor stations. The seasonal periods for each station can be calculated by the frequency corresponded to peak points. In order to reach a compromise between accuracy and complexity of model, amplitudes of all peak points in each station is sorted from large to small separately. Frequencies whose amplitudes account for 80% of total is chosen and turned to periods (1/ frequency), which are included in modified log-linear model.

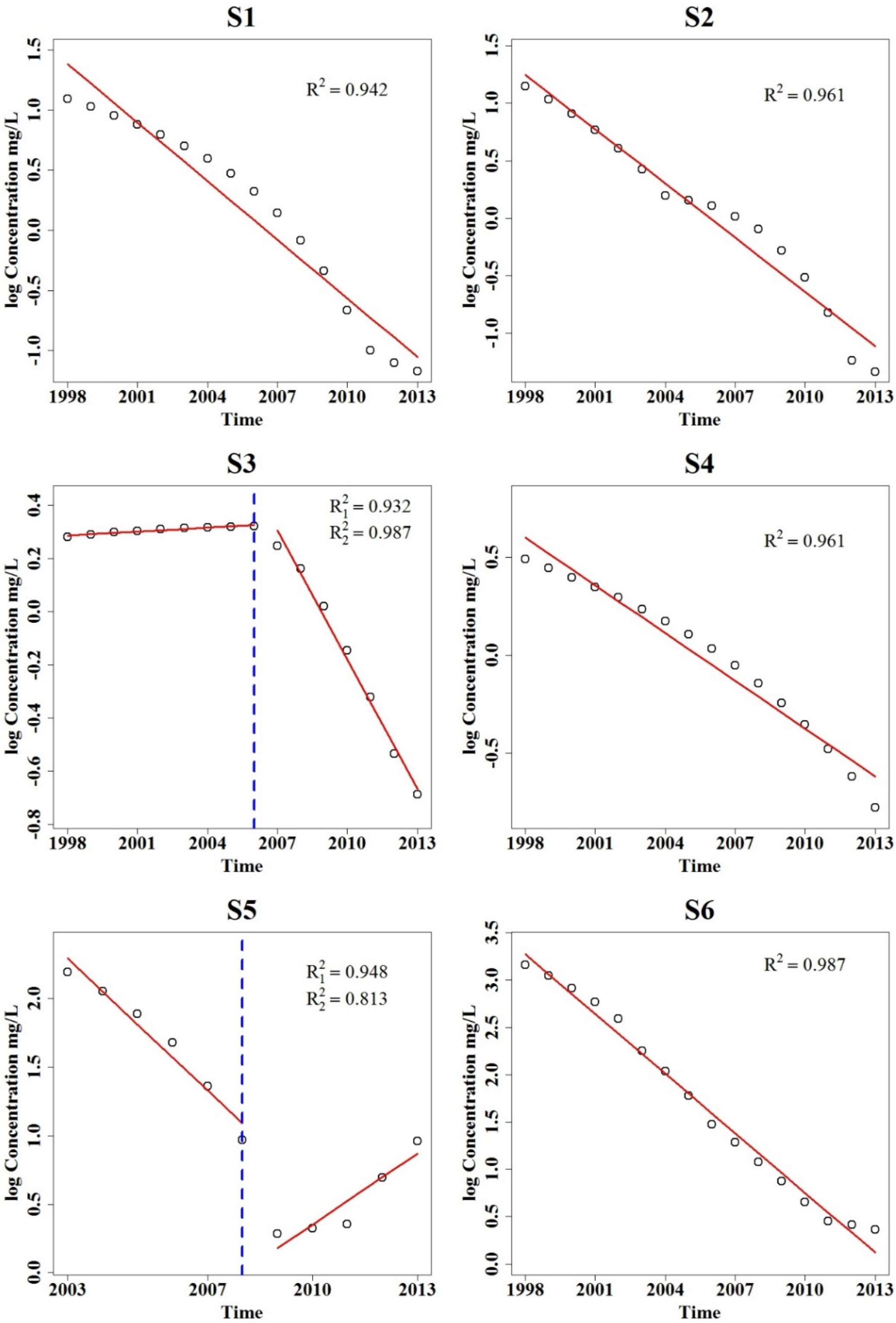
S1
$R^2 = 0.942$
S2
$R^2 = 0.961$
S3
$R_1^2 = 0.932$
$R_2^2 = 0.987$
S4
$R^2 = 0.961$
S5
$R_1^2 = 0.948$
$R_2^2 = 0.813$
S6
$R^2 = 0.987$
log Concentration mg/L
Time
1998
2001
2004
2007
2010
2013
2003

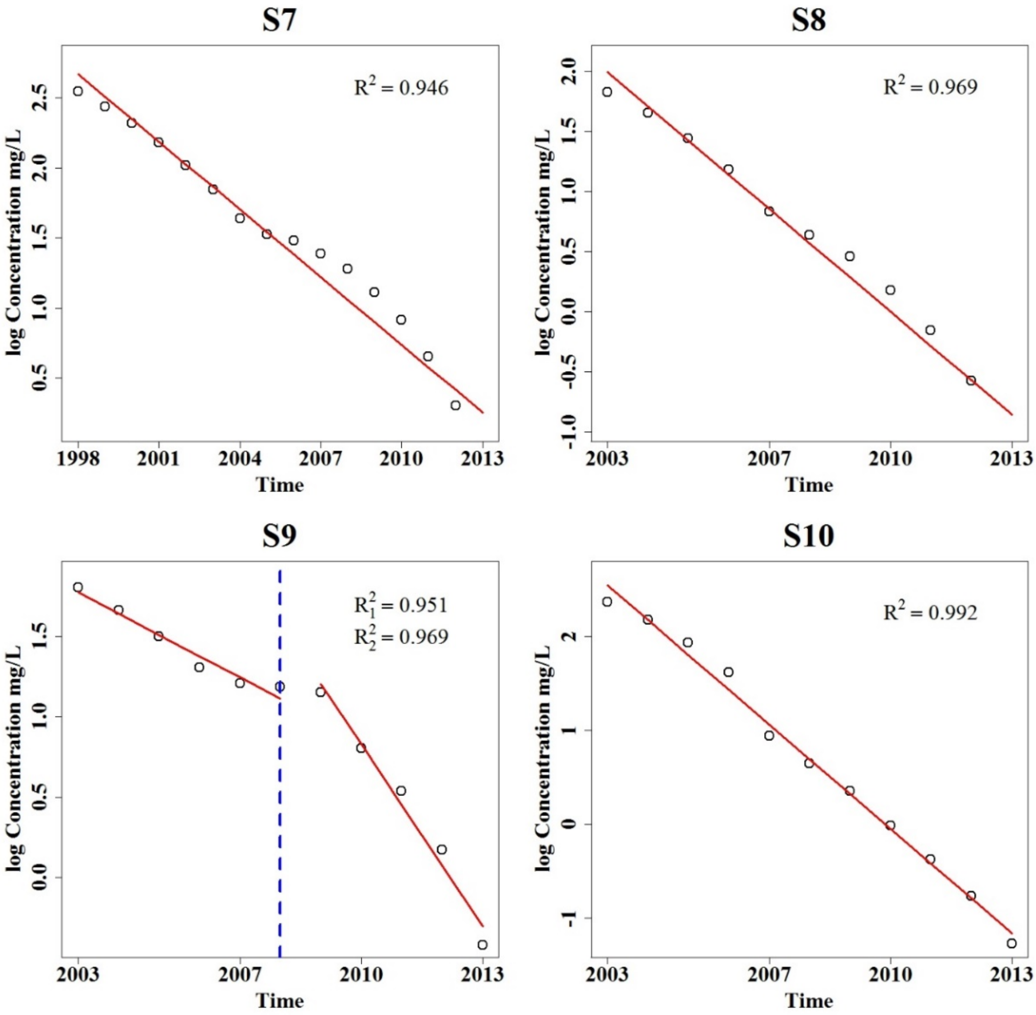

Figure 4. Amplitudes of seasonal components from the STL.

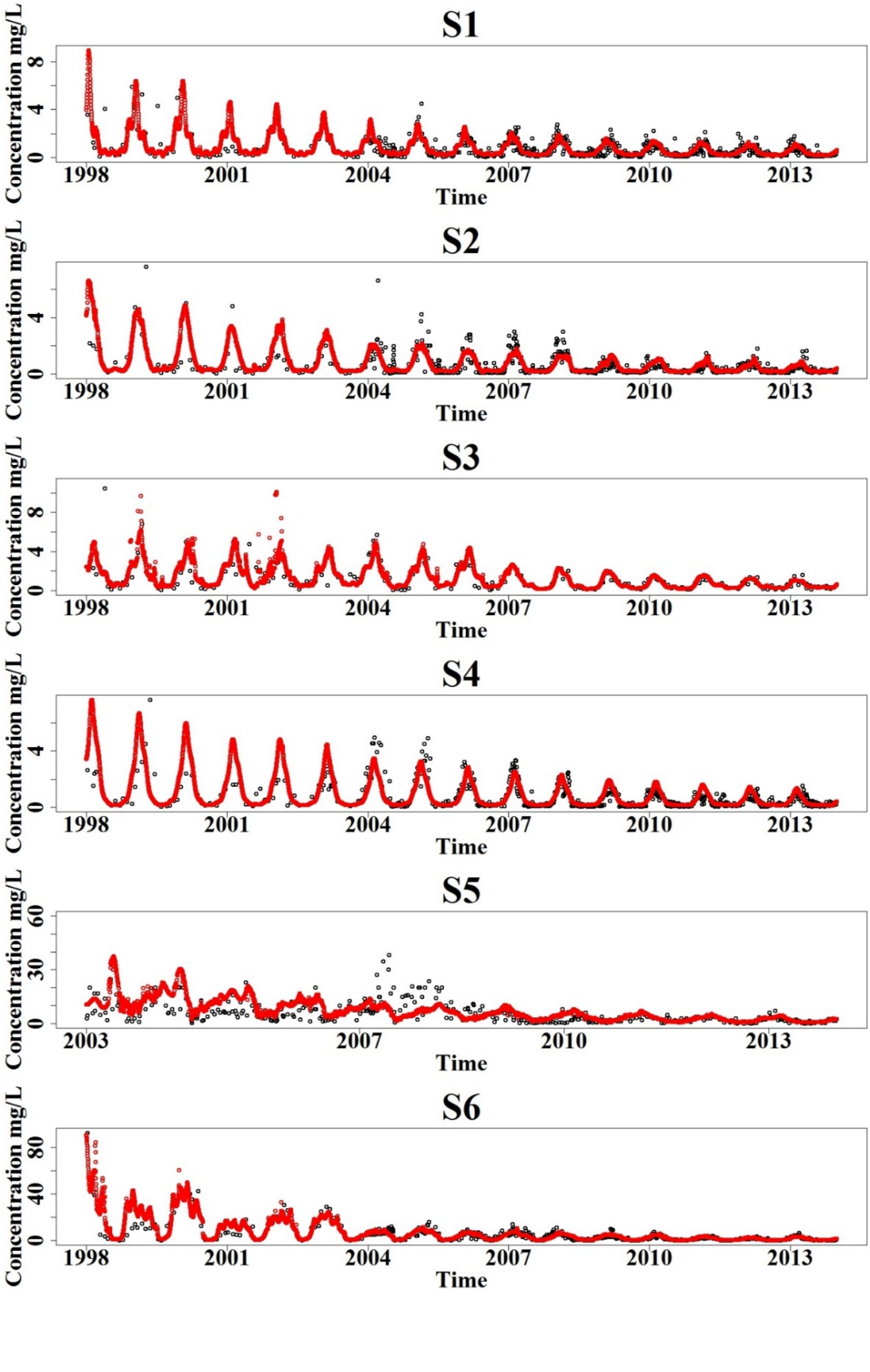
S1
Concentration mg/L
0
4
8
1998
2001
2004
2007
2010
2013
Time
S2
Concentration mg/L
0
4
1998
2001
2004
2007
2010
2013
Time
S3
Concentration mg/L
0
4
8
1998
2001
2004
2007
2010
2013
Time
S4
Concentration mg/L
0
4
1998
2001
2004
2007
2010
2013
Time
S5
Concentration mg/L
0
30
60
2003
2007
2010
2013
Time
S6
Concentration mg/L
0
40
80
1998
2001
2004
2007
2010
2013
Time

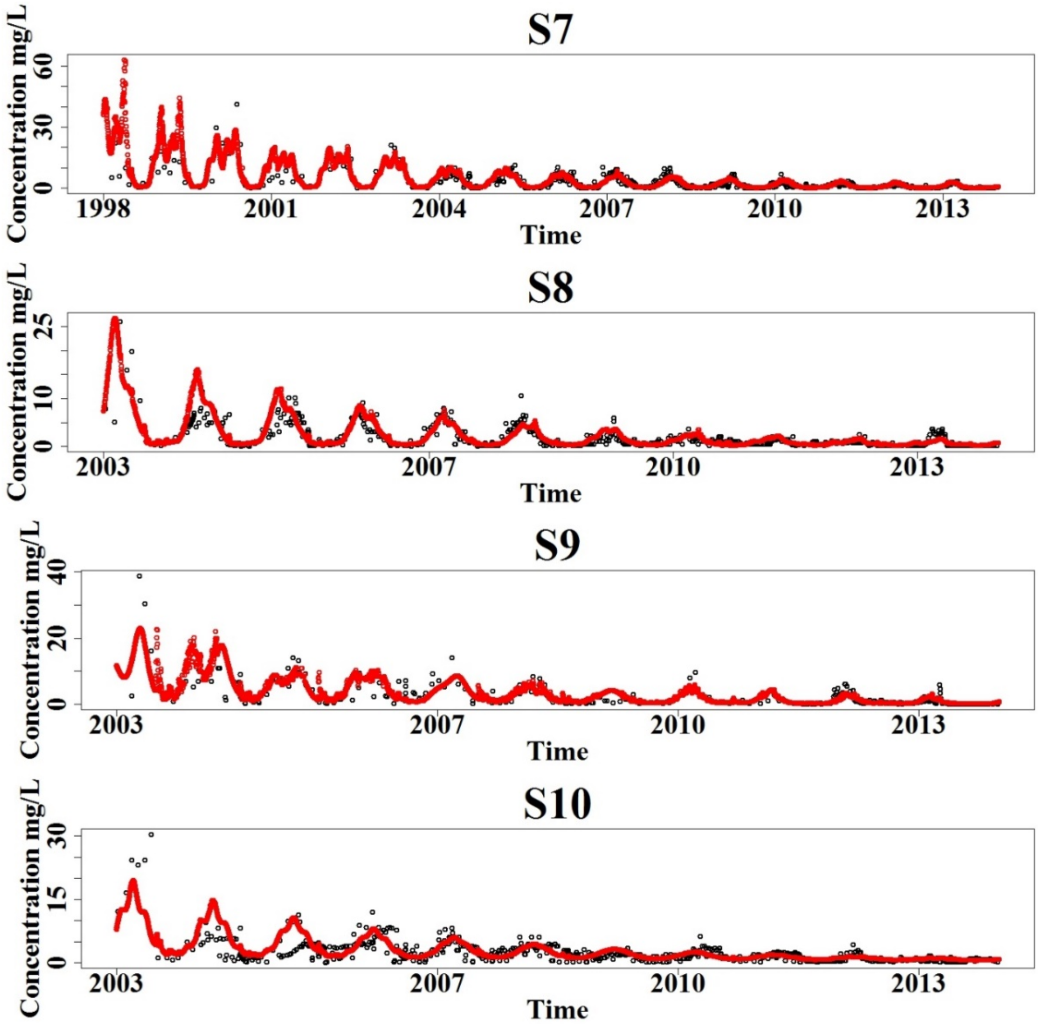

Figure 5. Value of sampling data and daily data interpolated by modified log-linear model of AN concentration in ten monitor stations. Sampling data and daily data is shown by black and red points respectively.

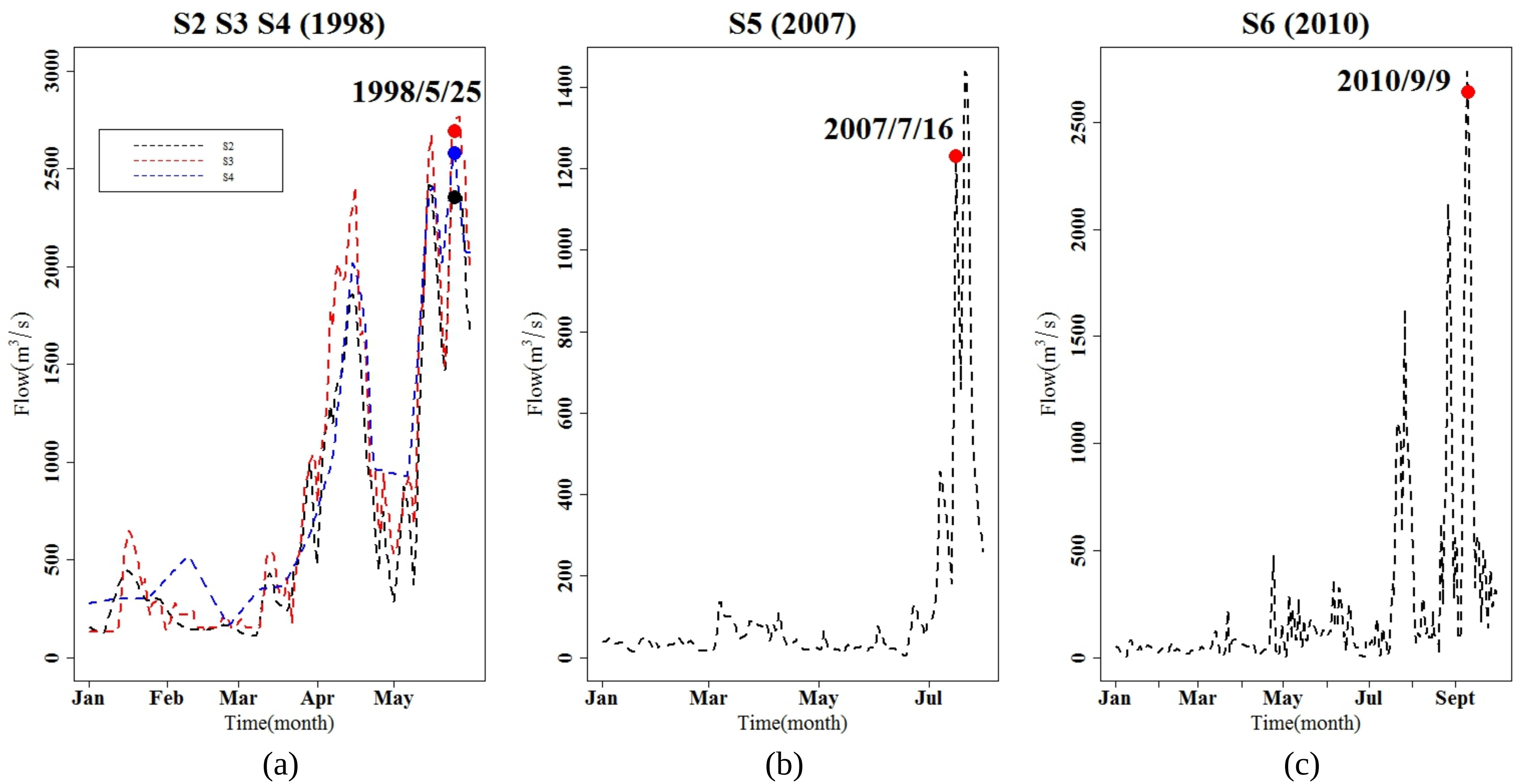

Figure 6. The flow values correspond to outliers in S2, S3, S4 in 1998, S5 in 2007 and S6 in 2010. In (a), black, red and blue lines represent flow in S2, S3 and S4 in 1998 respectively.

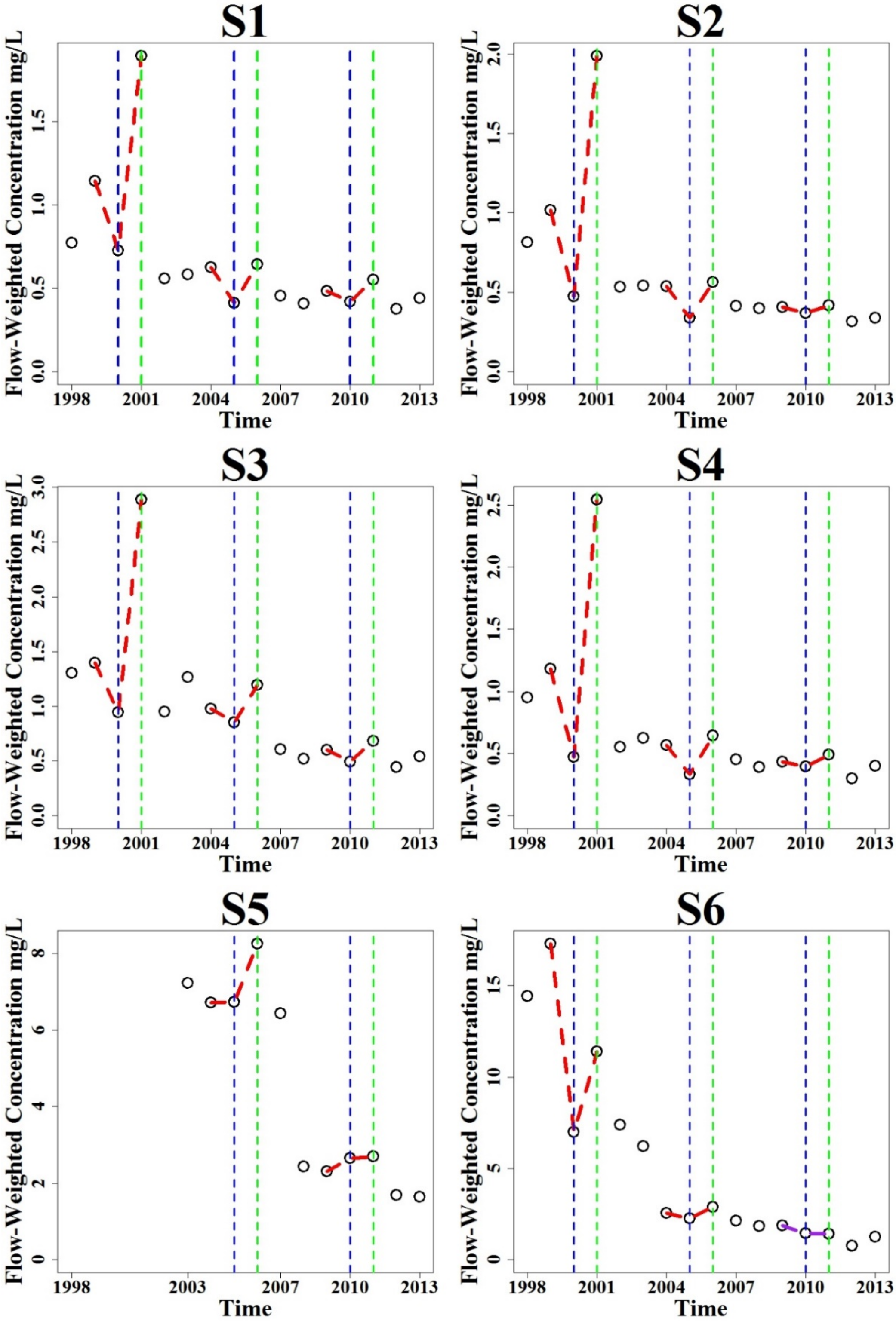
S1
S2
S3
S4
S5
S6
Flow-Weighted Concentration mg/L
Time
1998
2001
2003
2004
2007
2010
2013

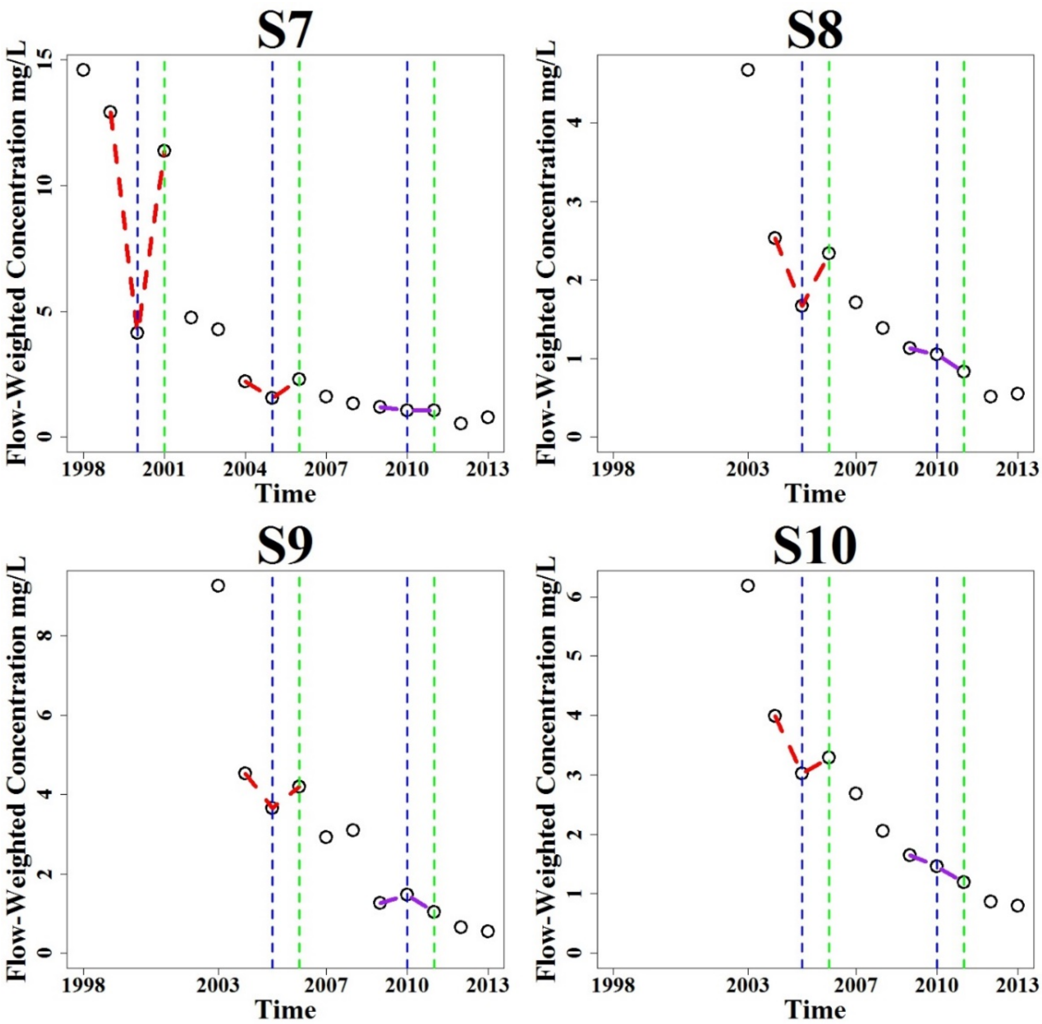

Figure 7. Average annual of AN flow-weighted concentration is calculated by annual total AN loads divided by annual total flow which is shown as black circles. Blue and green dotted lines are the last year of a Five-year Plan (2000, 2005, 2010) and the first year of next Five-year Plan (2001, 2006, 2011), respectively.

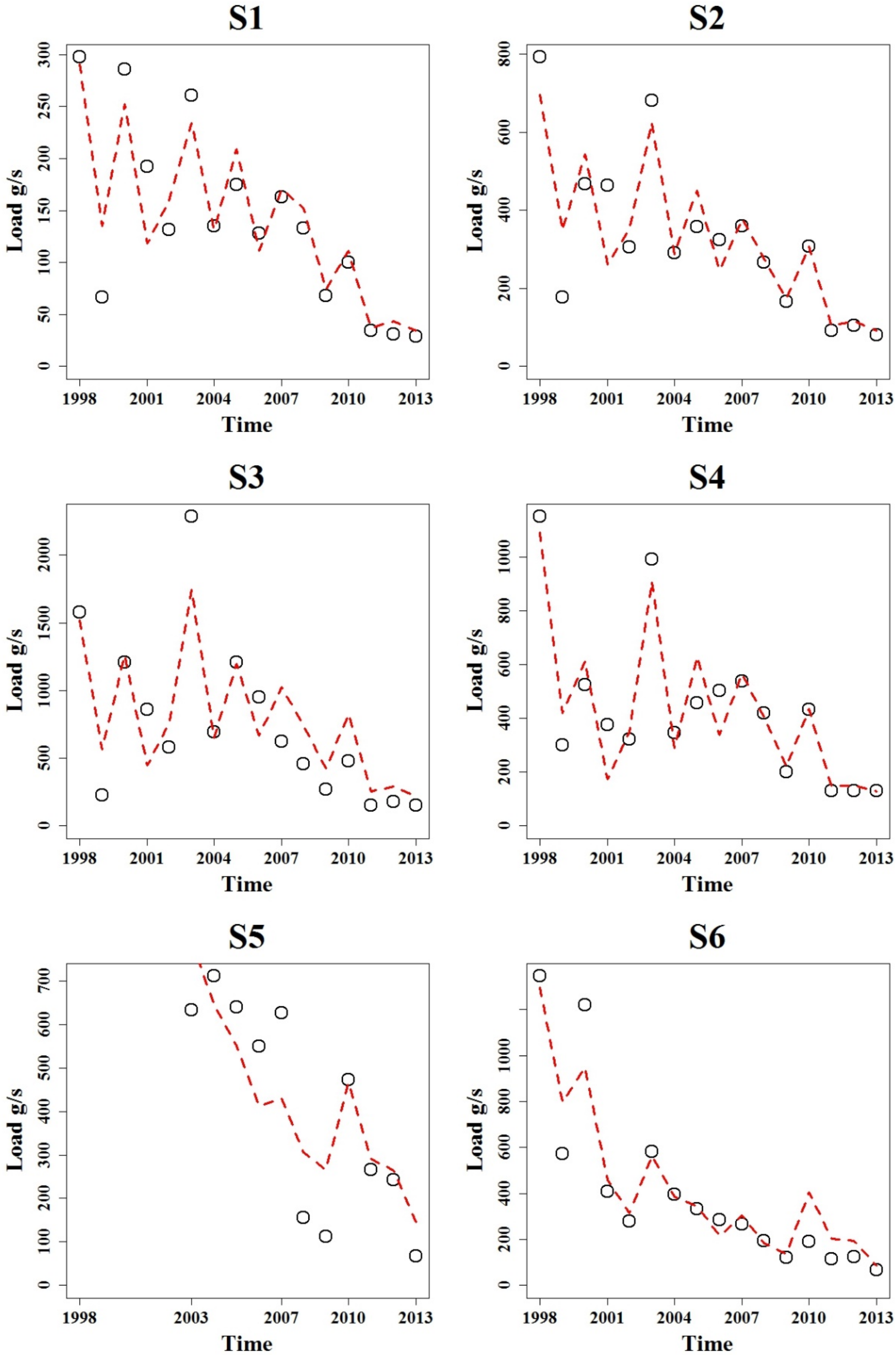
S1
Load g/s
Time
S2
Load g/s
Time
S3
Load g/s
Time
S4
Load g/s
Time
S5
Load g/s
Time
S6
Load g/s
Time

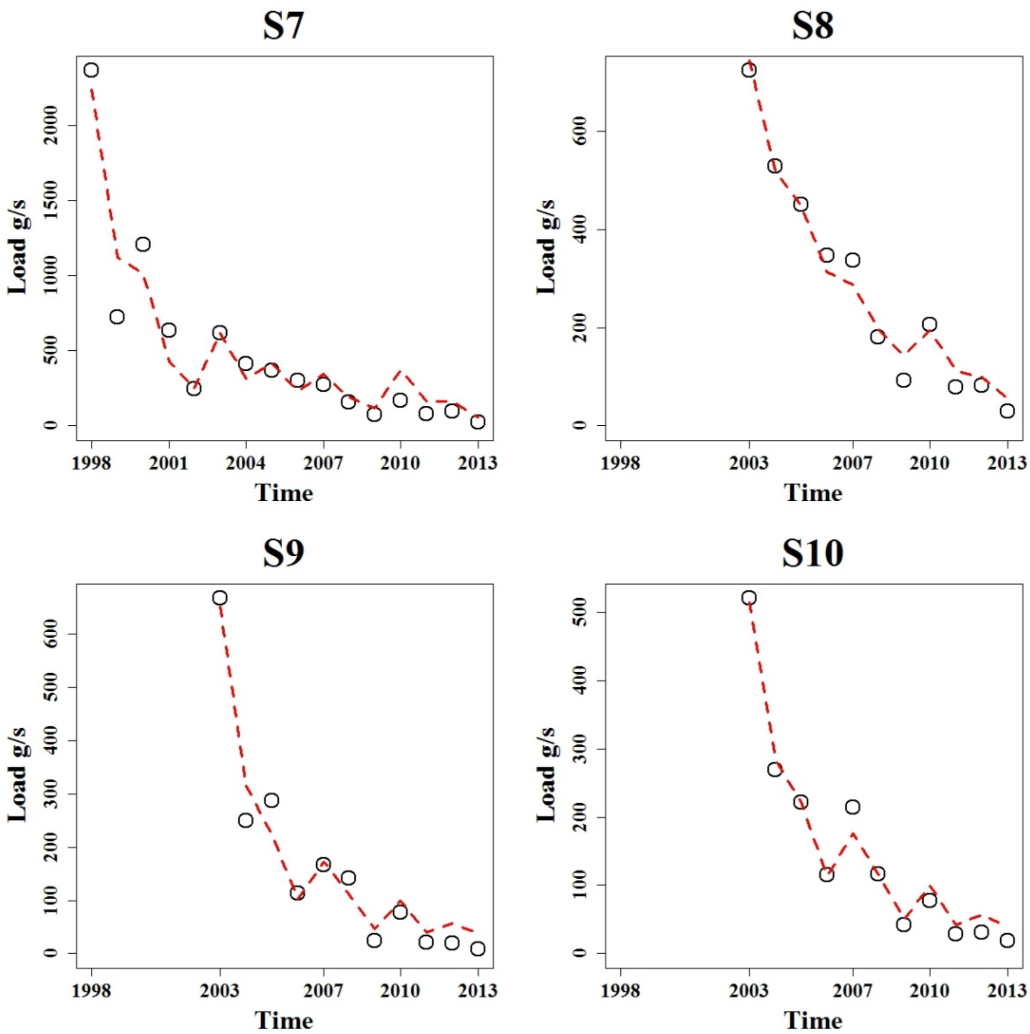

Figure 8. Average annual of AN loads and fitting lines. Average annual of AN loads and fitting AN loads is shown by black circles and red dotted lines, respectively.

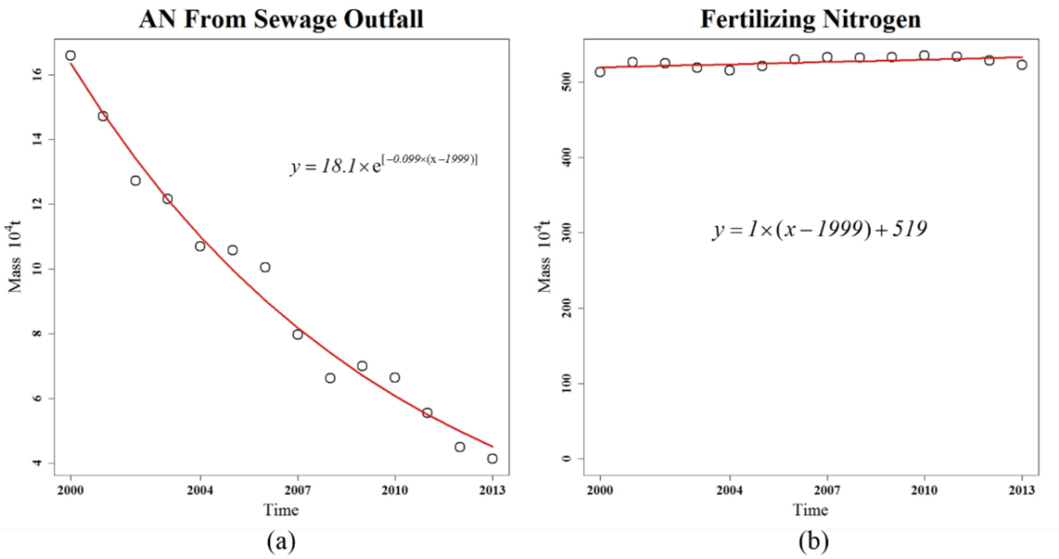

Figure 9. Annual total AN mass from sewage outfall (a) and mass of fertilizing nitrogen (b) in the HRB.

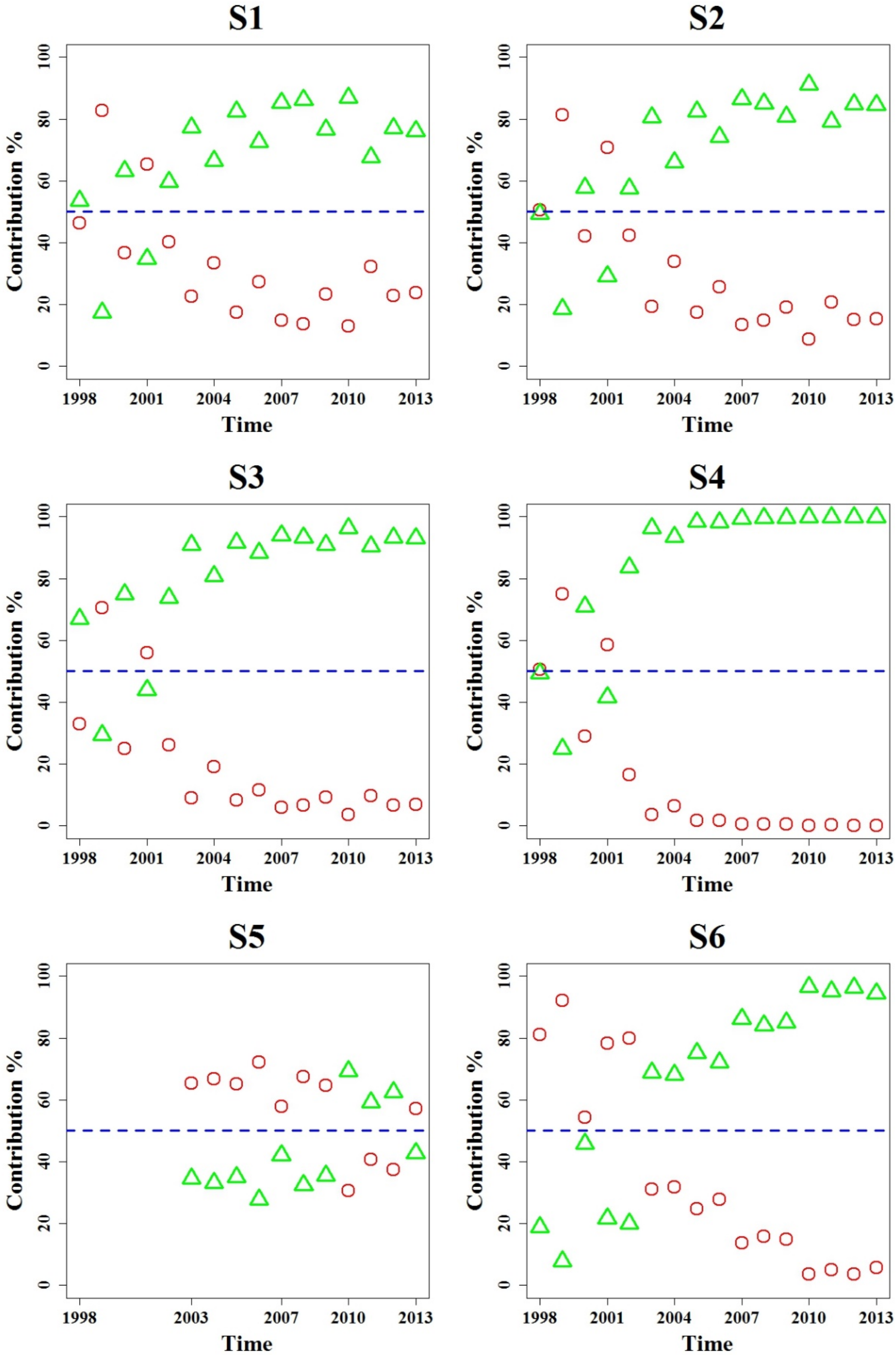
S1
S2
S3
S4
S5
S6
Contribution %
Time
0
20
40
60
80
100
1998
2001
2003
2004
2007
2010
2013

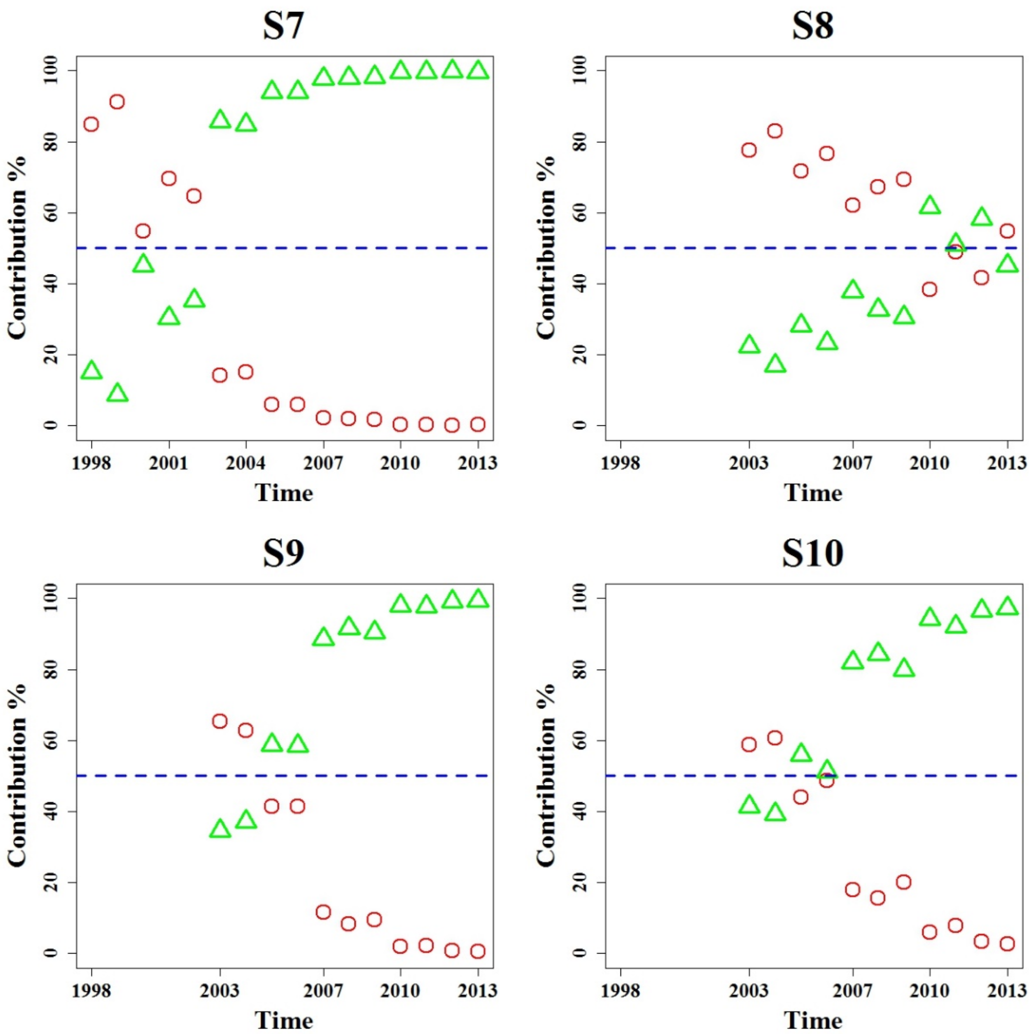

Figure 10. Contribution of AN loads from point and non-point sources in ten monitor stations. Point and non-point sources are shown by red circles and green triangles, respectively.